INTERNATIONAL JOURNAL OF Experimental Pathology

Int. J. Exp. Pathol. (2015), 96, 319–325

ORIGINAL ARTICLE

Altered expression of CKs 14/20 is an early event in a rat model of multistep bladder carcinogenesis

Rui M. Gil da Costa*,†,1, Paula A. Oliveira‡,§,1, Carmen Vasconcelos-Nóbrega¶,**, Regina Arantes-Rodrigues§, Rosário Pinto-Leite††, Aura A. Colaço‡,‡‡, Luis F. de la Cruz§§ and Carlos Lopes†

**LEPABE, Departamento de Engenharia Química, Faculdade de Engenharia da Universidade do Porto (FEUP), Porto, Portugal, †Grupo de Patologia e Terapêutica Experimental, CI-IPOP, Instituto Português de Oncologia, Porto, Portugal, ‡Departamento de Ciências Veterinárias, Universidade de Trás-os-Montes e Alto Douro (UTAD), Vila Real, Portugal, §CITAB, UTAD, Vila Real, Portugal, ¶Instituto Politécnico de Viseu, Escola Agrária de Viseu, Viseu, Portugal, **CECA, Universidade do Porto, Porto, Portugal, ††Laboratorio de Citogenética, Departamento de Genética Humana, Centro Hospitalar de Trás-os-Montes e Alto Douro, Vila Real, Portugal, ‡‡ECAV, UTAD, Vila Real, Portugal and §§Departamento de Fisiologia, Faculdade de Veterinária, Universidade de Santiago de Compostela, Lugo, Spain*

INTERNATIONAL JOURNAL OF EXPERIMENTAL PATHOLOGY

doi: 10.1111/iep.12145

Received for publication: 25 February 2015
Accepted for publication: 22 July 2015

Correspondence:
Rui M. Gil da Costa
Departamento Engenharia Química
FEUP
Rua Dr. Roberto Frias
4200-465 Porto
Portugal
Tel.: +351 225081400
Fax: +351 22 508 14 40
E-mail: rmcosta@fe.up.pt
and
Paula A. Oliveira
Departamento de Ciências Veterinárias
UTAD
Quinta de Prados
5000-911 Vila Real
Portugal
Tel.: +351 259350651
Fax: +351 259 350 480
E-mail: pamo@utad.pt

[1]Both authors contributed equally to this work.

SUMMARY

Cytokeratins (CKs) 14 and 20 are promising markers for diagnosing urothelial lesions and for studying their prognosis and histogenesis. This work aimed to study the immunohistochemical staining patterns of CK14/20 during multistep carcinogenesis leading to papillary bladder cancer in a rat model. Thirty female Fischer 344 rats were divided into three groups: group 1 (control); group 2, which received N-butyl-N-(4-hydroxybutyl)nitrosamine (BBN) for 20 weeks plus 1 week without treatment; and group 3, which received BBN for 20 weeks plus 8 weeks without treatment. Bladder lesions were classified histologically. CK14 and CK20 immunostaining was assessed according to its distribution and intensity. In control animals, 0–25% of basal cells and umbrella cells stained positive for CK14 and CK20 respectively. On groups 2 and 3, nodular hyperplastic lesions showed normal CK20 and moderately increased CK14 staining (26–50% of cells). Dysplasia, squamous metaplasia, papilloma, papillary tumours of low malignant potential and low- and high-grade papillary carcinomas showed increased CK14 and CK20 immunostaining in all epithelial layers. Altered CK14 and CK20 expression is an early event in urothelial carcinogenesis and is present in a wide spectrum of urothelial superficial neoplastic and preneoplastic lesions.

Keywords
bladder cancer, CK14, CK20, multistep carcinogenesis, rat, stem cell

Bladder cancer, with its high incidence and recurrence rates, constitutes one of the most challenging problems in the field of oncology. Extensive studies have addressed the biopathology of urothelial neoplasms, trying to identify new therapeutic targets or better prognostic markers. Among these, some cytoskeletal proteins of the cytokeratin (CK) family have

shown significant associations with response to therapy and disease outcome. Such CKs are normally restricted to specific cell populations within the urothelium; for example, CKs 5, 6 and 14 are restricted to the basal cell layer and CK20 to the superficial umbrella cells (Reedy *et al.* 1990; Ramos *et al.* 2003; revised by Ho *et al.* 2012). Altered expression of these markers – that is their presence in cell layers where they are normally absent – reflects aberrant differentiation during the complex process of urothelial carcinogenesis. CK20 and the basal component markers CK5/6 are helpful in distinguishing reactive urothelial atypia from urothelial neoplasia (Edgecombe *et al.* 2012; Amin *et al.* 2014). Altered CK20/14 expression significantly correlates with worsened prognosis. Ramos *et al.* (2003) described an association between increased CK20 expression and disease recurrence in patients with low-grade papillary tumours. Aberrant CK20 expression was also correlated with increased Ki-67 counts, as well as with tumour stage, histological grade, the presence of metastasis and reduced progression-free survival (Ye *et al.* 2010). Otto *et al.* (2013) recently reported that increased CK20 expression correlated with shorter recurrence-free survival in patients with T1 urothelial bladder carcinoma. Aberrant CK14 expression was also recently associated with shorter overall survival in patients with bladder cancer (Volkmer *et al.* 2012). However, although the role of these markers in the prognosis of cancer is increasingly accepted, the underlying mechanisms in terms of tumour histogenesis remain largely obscure. Urothelial cancer often shows a poorly differentiated, stem-cell-like phenotype, which has been proposed to arise from normal urothelial stem cells, or de-differentiation of mature cells in the course of carcinogenesis (Hatina & Schulz 2012; Ho *et al.* 2012; Volkmer *et al.* 2012). One of the most useful and commonly used tools for studying bladder carcinogenesis is the N-butyl-N-(4-hydroxybutyl)nitrosamine (BBN)-induced rat model, which recapitulates the multistep process leading to papillary urothelial neoplasms (Vasconcelos-Nóbrega *et al.* 2012). Compared with tumour samples from patients with cancer, this model offers the possibility to study the histogenesis of bladder lesions during the multistep carcinogenesis process over a relatively short period of time. This model originates papillary lesions which closely resemble their human counterparts, both morphologically and molecularly (Arantes-Rodrigues *et al.* 2013). Accordingly, we have elected this model to study the expression of CKs 14 and 20 during multistep bladder carcinogenesis.

Materials and methods

Animals and experimental procedures

Thirty female 5-week-old Fischer 344 rats (Harlan) were housed in the animal facilities of the University of Trás-os-Montes and Alto Douro. All procedures involving the animals were performed in accordance with European Directive 2010/63/EU and established guidelines, after approval by the Portuguese Ethics Committee for Animal Experimentation (Direcção Geral de Alimentação e Veterinária, Approval No. 520/000/000/2003). The animals were kept in quarantine for 1 week and then in ventilated chambers, under controlled conditions of temperature (23 ± 2°C), light–dark cycle (12-h light/12-h dark) and humidity (50 ± 10%), using hardwood bedding (Mucedola). A standard diet (Global Diet 2014; Harlan, Barcelona, Spain) and water were provided *ad libitum*. N-(4-hydroxybutyl)nitrosamine was administered in the drinking water at a concentration of 0.05%, using light-protected bottles. The animals were randomly divided into three groups: group 1 (control), which received untreated water; group 2, which received BBN-treated water for 20 weeks plus 1 week without treatment; group 3, which received BBN-treated water for 20 weeks plus 8 weeks without treatment. At the end of the experimental protocol, all animals were sacrificed by means of a lethal intraperitoneal pentobarbital injection (100 mg/kg) and necropsied. Urinary bladders were fixated *in situ* with 10% neutral buffered formalin through the urethra (300 μl) for 24 h and routinely processed for histological analysis.

Histological and immunohistochemical analysis

Urinary bladder lesions were classified histologically using haematoxylin and eosin-stained slides. Immunohistochemistry for CK14 (1:20; NCL-L-LL002; Novocastra, Newcastle upon Tyne, UK) and CK20 (1:25; Ks20.8; M7019; Dako, Glostrup, Denmark) was performed on 2-μm-thick sections. Heat-induced epitope retrieval was performed in a microwave oven (700 W) for 20 min in a citrate buffer solution. Endogenous peroxidase activity was blocked with 3% hydrogen peroxide. Non-specific staining was minimized by a 30-min incubation with normal rabbit serum (X 0902; DakoCytomation, Glostrup, Denmark). Each primary antibody was incubated overnight (4°C) in a humid chamber. Immunoreactivity was detected using a biotin-labelled anti-mouse secondary antibody (1:400, E 0354; DakoCytomation), followed by a streptavidin–biotin–peroxidase complex (TS-

Table 1 Incidence of N-butyl-N-(4-hydroxybutyl)nitrosamine-induced rat bladder lesions

	Group 1	Group 2	Group 3
Lesions	**No. of lesions**		
Normal (n = 10)	10		
Nodular hyperplasia (n = 18)		8	10
Dysplasia (n = 20)		10	10
Squamous metaplasia (n = 14)		7	7
Papilloma (n = 6)		3	3
Papillary tumour of low malignant potential (n = 10)		4	6
Low-grade papillary carcinoma (n = 20)		11	9
High-grade papillary carcinoma (n = 8)			8

125-HR; LabVision Corporation, Fremont, CA, USA) and colour development using 3,3′-diaminobenzidine tetrahydrochloride. For negative controls, sections were incubated with normal rabbit serum instead of the primary antibody. Skin squamous epithelium was used as positive control. Immunostaining for each marker was assessed according to its distribution and intensity. Concerning the distribution of positive cells, four staining patterns were observed: pattern I, comprising cases where immunostaining was present in less than 25% of urothelial cells; pattern II with 26–50% of stained cells; pattern III with 51–75% of stained cells; and pattern IV with 76–100% of stained cells. The staining intensity was scored as light, moderate or intense.

Results

Tumour induction

No lesions were observed in control (group 1) animals. Macroscopically exposed animals (groups 2 and 3) showed

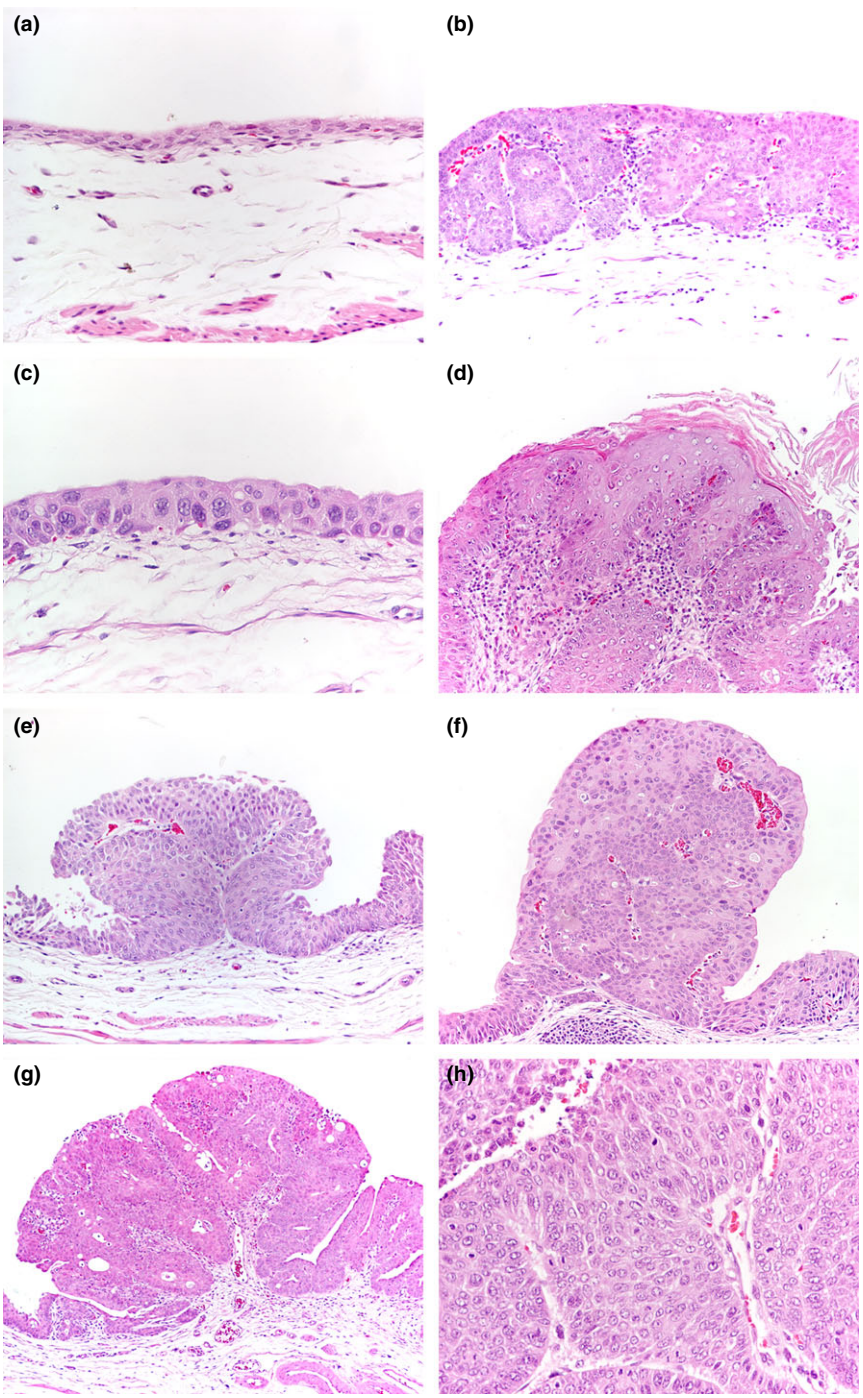

Figure 1 N-butyl-N-(4-hydroxybutyl) nitrosamine-induced rat bladder lesions. (a) Control animal. Normal bladder urothelium (100×). (b) Nodular hyperplasia (nh, 40×). (c) Urothelial dysplasia (d, 400×). (d) Squamous metaplasia (sqm, 200×). (e) Urothelial papilloma (pap, 100×). (f) Papillary tumour of low malignant potential (ptlmp, 100×). (g) Low-grade urothelial carcinoma (lgpc, 40×). h, high-grade papillary carcinoma (hgpc, 400×).

Table 2 Immunohistochemical staining patterns for CKs 14 and 20 in N-butyl-N-(4-hydroxybutyl)nitrosamine induced rat bladder lesions

	CK14 (% of lesions)				CK20 (% of lesions)			
Lesions (*n*)	I	II	III	IV	I	II	III	IV
Normal (*n* = 10)	100				100			
nh (*n* = 18)		75	25		100			
d (*n* = 20)		11	72	17		33	59	8
sqm (*n* = 14)				100		55	27	18
pap (*n* = 6)			17	83			50	50
ptlmp (*n* = 10)			44	56		60	40	
lgpc (*n* = 20)		18	47	35			83	17
hgpc (*n* = 8)			62	38			100	

CK, cytokeratin; nh, nodular hyperplasia; d, dysplasia; sqm, squamous metaplasia; pap, papilloma; ptlmp, papillary tumour of low malignant potential; lgpc, low-grade papillary carcinoma; hgpc, high-grade papillary carcinoma.

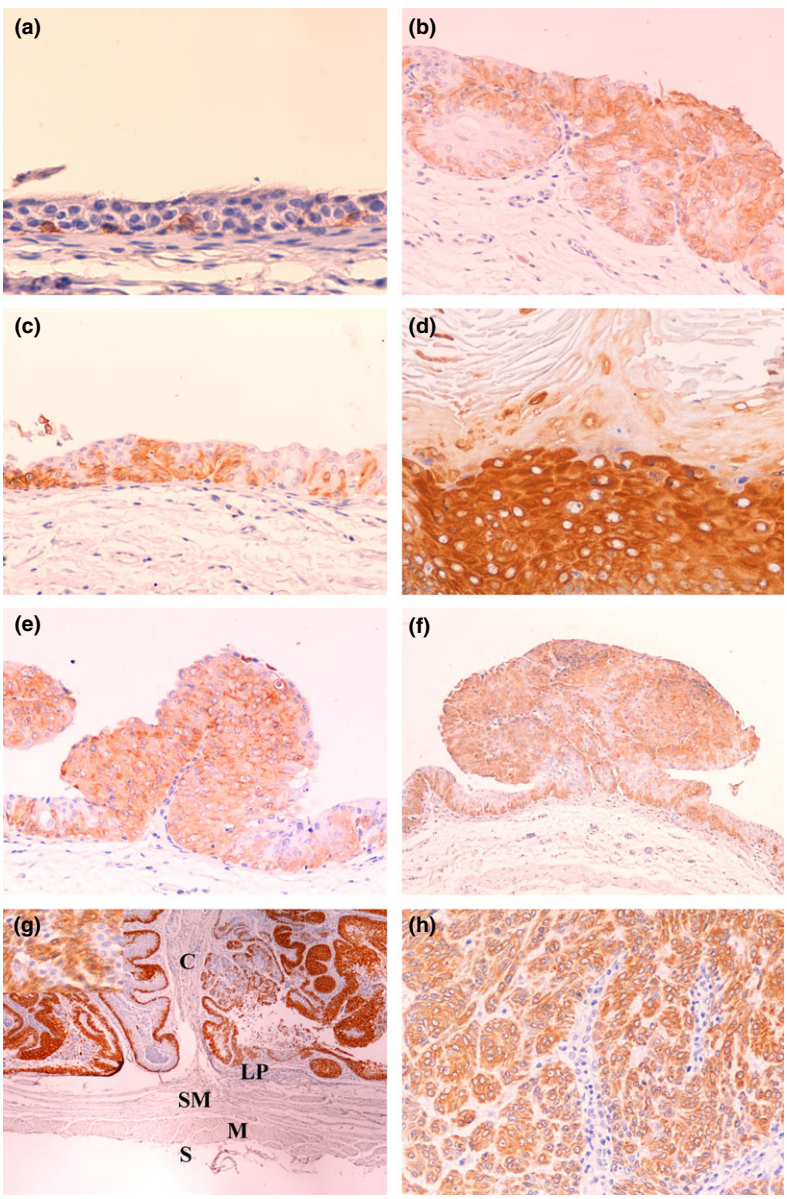

Figure 2 CK14 immunostaining in N-butyl-N-(4-hydroxybutyl)nitrosamine-induced rat bladder lesions. (a) Control animal. Normal bladder urothelium (400×). Note immunostaining restricted to scattered basal cells. (b) Nodular hyperplasia (nh, 200×). Note diffuse immunostaining. (c) Urothelial dysplasia (d, 200×). Note immunostaining in the full thickness of the urothelium. (d) Squamous metaplasia (sqm, 200×). Note intense immunostaining. (e) Urothelial papilloma (pap, 200×). (f) Papillary tumour of low malignant potential (ptlmp, 40×). (g) Low-grade papillary carcinoma: C, carcinoma; LP, *lamina propria*; SM, *lamina submucosa*; M, *lamina muscularis*; S, *lamina serosa* (lgpc, 40×). The upper left corner inset is a high-power image of the same lesion (400×). (h) High-grade papillary carcinoma (hgpc, 400×). Note variably intense, diffuse staining of lesions e–h.

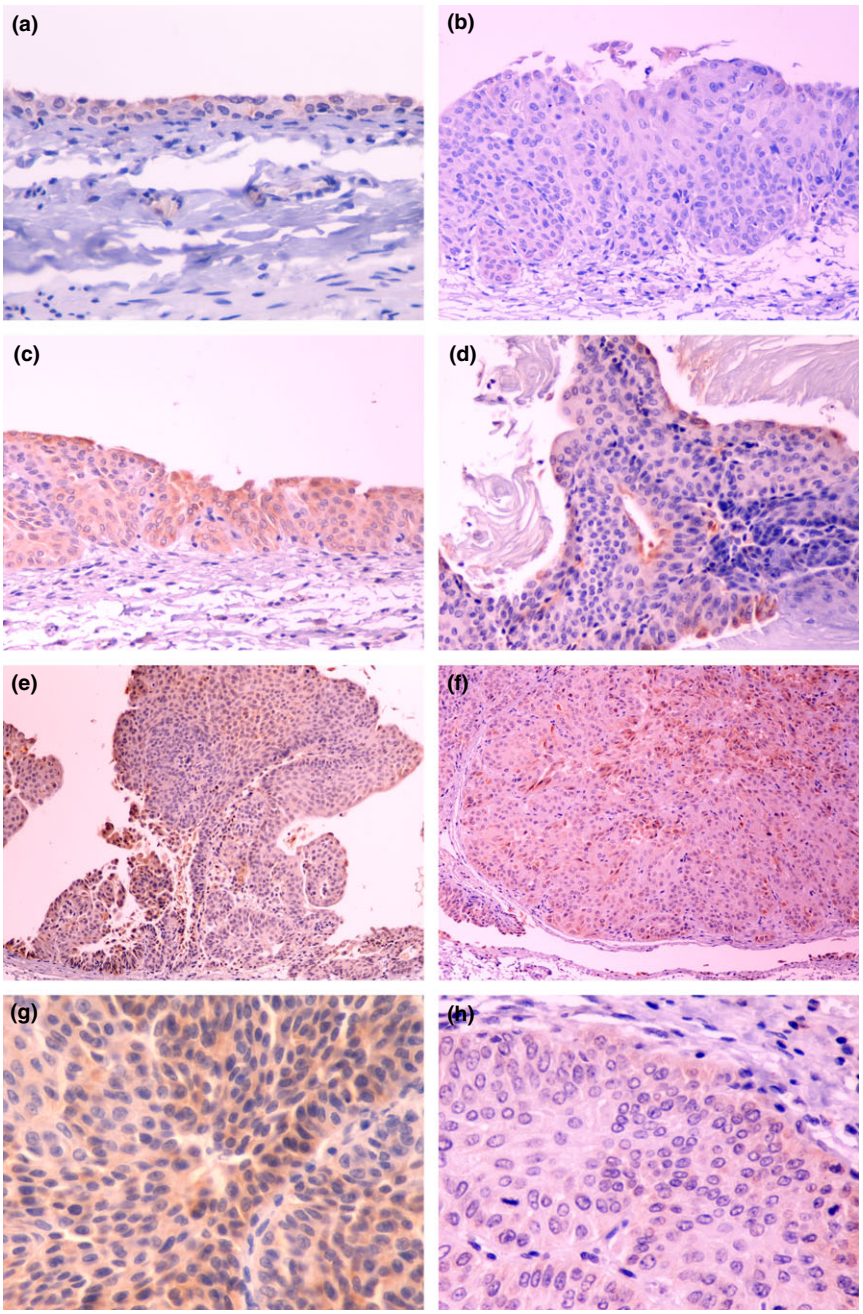

Figure 3 CK20 immunostaining in N-butyl-N-(4-hydroxybutyl)nitrosamine-induced rat bladder lesions. (a) Control animal. Normal bladder urothelium (400×). Note immunostaining restricted to umbrella cells. (b) Nodular hyperplasia (nh, 200×). CK20 immunostaining is absent. (c) Urothelial dysplasia (d, 200×). Note immunostaining in the full thickness of the urothelium. (d) Squamous metaplasia (sqm, 200×). Note immunostaining restricted to superficial cells. (e) Urothelial papilloma (pap, 100×). (f) Papillary tumour of low malignant potential (ptlmp, 100×). (g) Low-grade urothelial carcinoma (lgpc, 400×). (h) High-grade papillary carcinoma (hgpc, 400×). Note variably intense, diffuse staining of lesions e–h.

enlarged, thickened and congested bladders showing multiple proliferative papillary luminal lesions. Urothelial lesions were classified histologically as nodular hyperplasia (nh), dysplasia (d), squamous metaplasia (sqm), papilloma (pap), papillary tumour of low malignant potential (ptlmp), low-grade papillary carcinoma (lgpc) and high-grade papillary carcinoma (hgpc) (Table 1 and Figure 1). High-grade papillary carcinomas were restricted to group 3 animals, with the longer incubation period following BBN exposure.

CK14 and CK20 immunoexpression

Among control (group 1) animals showing normal bladder histology, the expression of CK14 and CK20 was light to moderate and restricted to 0–25% (pattern I) of basal and umbrella cells respectively (Table 2 and Figures 2 and 3). Nodular hyperplastic areas showed normal CK20 and increased CK14 expression (patterns II and III). All other lesions showed increased CK14 expression with moderate-to-intense staining and increased numbers of positive cells in

all epithelial cell layers (patterns II to IV). Similar changes were observed for CK20, although the staining intensity was generally higher among superficial cells compared with lower epithelial layers.

Discussion

Evidence accumulated in recent years shows that the urothelium is a hierarchically organized epithelium that develops according to a strict differentiation programme and contains more than one tissue-specific stem-cell population (Hatina & Schulz 2012; Ho *et al.* 2012). Not surprisingly, urothelial lesions retain morphological and molecular features of urothelial differentiation, such as the expression of cell-type-specific CKs (Ramos *et al.* 2003; Hodges *et al.* 2010; Mai *et al.* 2013; Choi *et al.* 2014). Experimental models are necessary to investigate the histogenesis of bladder cancer, as reviewed by Oliveira *et al.* (2014), complementing the data obtained with tumour samples from patients with cancer. Some animal models, such as BBN-induced bladder tumours obtained in rats and mice, provide a realistic, multistep approach to carcinogenesis, in the setting of an immunocompetent organism. Other models, relying on bladder cancer cell lines xenografted into immunodeficient mice, lack these characteristics. The rat and mouse models are complementary: while rats typically develop papillary tumours in response to BBN, mice develop invasive lesions (Vasconcelos-Nóbrega *et al.* 2013; Oliveira *et al.* 2014).

Now, for the first time, we traced the expression of CK14 and CK20 during the consecutive steps of BBN-induced carcinogenesis in the rat bladder. A number of different steps were identified, starting from urothelial hyperplasia, followed by dysplasia, papillomas, ptlmp, lgpc and hgpc (Table 1). Importantly, aberrant CK14 and CK20 immunoexpression was consistently present in the early steps of neoplastic transformation, such as dysplastic lesions, and was maintained in papillomas, ptlmp, lgpc and hgpc (Table 2). Differently, hyperplastic lesions seemed to consist essentially of a basal cell proliferation, showing orderly differentiation towards the superficial umbrella cells. Our results agree with the fact that CK14 has been considered the most primitive marker of urothelial differentiation (Volkmer *et al.* 2012). The areas of squamous differentiation showed intense CK14 but little CK20 immunostaining, in agreement with previous clinical and experimental findings (Harnden & Southgate 1997; Gee *et al.* 2003; Liang *et al.* 2005). These lesions, often associated with trematode infestations in patients with cancer, thus seem to have distinctive molecular features. The more advanced lesions, ptlmp, lgpc and hgpc, showed a patchy, heterogeneous immunostaining for both markers. This is consistent with the characteristic heterogeneity frequently observed in patients with cancer. CKs 14 and 20 have been used to distinguish between morphologically related lesions and were shown to correlate with tumour prognosis. In our experimental model, altered CK14/20 staining was associated with multiple preneoplastic and neoplastic lesions. This agrees with the findings from clinical studies correlating aberrant CK14/20 staining with worsened prognostic in patients with bladder cancer (Ramos *et al.* 2003; Ye *et al.* 2010; Volkmer *et al.* 2012; Otto *et al.* 2013). The present results may also support the use of CK20 for distinguishing neoplastic and preneoplastic foci from some reactive lesions, as previously proposed (Edgecombe *et al.* 2012; Amin *et al.* 2014). However, similar expression patterns for both markers were observed in lgpc and hgpc, contrasting with previous findings from clinical studies (Mumtaz *et al.* 2014).

Employing this rat model, we previously reported that increasingly more aggressive lesions show increased DNA aneuploidy rates, Ki-67 (Palmeira *et al.* 2009) and p53 labelling indices (Oliveira *et al.* 2006a) and decreased E-cadherin expression (Oliveira *et al.* 2006b). Taking both the previous and present results together, a picture emerges in which modest DNA aneuploidy and aberrant CK14/20 expression are early events of multistep carcinogenesis leading to papillary bladder cancer. Proliferation rates and DNA aneuploidy increase progressively in more aggressive lesions accompanied by altered p53 status, while the loss of E-cadherin expression appears as a later event in cancer progression.

Using the BBN-induced mouse model of invasive bladder cancer, Shin *et al.* (2014) recently traced the origin of those bladder lesions to a subset of basal urothelial stem cells. Bladder tumours expressed high levels of the basal marker CK5, while acquiring a heterogeneous phenotype, which is in accordance with our findings in the rat model of papillary cancer. The present results provide a comprehensive overview of the expression of CKs 14/20 along multistep carcinogenesis leading to papillary bladder cancer and pave the way for lineage-tracing studies, similar to those performed by Shin *et al.* (2014), which may clarify the histogenesis of this type of bladder cancer.

Acknowledgements

Rui M. Gil da Costa is supported by postdoctoral research grant SFRH/BPD/85462/2012, from the Portuguese Foundation for Science and Technology, funded by the Portuguese Government and the Social European Fund.

Conflict of Interest

The authors declare no conflicts of interest.

References

Amin N.B., Trpkov K, Lopez-Beltran A, Grignon D, Members of the ISUP Immunohistochemistry in Diagnostic Urologic Pathology Group. (2014) Best practices recommendations in the application of immunohistochemistry in the bladder lesions: report from the International Society of Urologic Pathology consensus conference. *Am. J. Surg. Pathol.* **38**, e20–e34.

Arantes-Rodrigues R., Pinto-Leite C.R., da Costa R.G., Colaço A., Lopes C. & Oliveira P. (2013) Cytogenetic characterization of an N-butyl-N-(4-hydroxybutyl) nitrosamine-induced mouse papillary carcinoma. *Tumour Biol.* **34**, 2691–2696.

Choi W., Czerniak B., Ochoa A. *et al.* (2014) Intrinsic basal and luminal subtypes of muscle-invasive bladder cancer. *Nat. Rev. Urol.* **11**, 400–410.

Edgecombe A., Nguyen B.M., Djordjevic B., Belanger E.C. & Mai K.T. (2012) Utility of cytokeratin 5/6, cytokeratin 20 and p16 in the diagnosis of reactive urothelial atypia and noninvasive component of urothelial neoplasia. *Appl. Immunohistochem. Mol. Morphol.* **20**, 264–271.

Gee J.R., Montoya R.G., Khaled H.M., Sabichi A.L. & Grossman H.B. (2003) Cytokeratin 20, AN43, PGDH, and COX-2 expression in transitional and squamous cell carcinoma of the bladder. *Urol. Oncol.* **21**, 266–270.

Harnden P. & Southgate J. (1997) Cytokeratin 14 as a marker of squamous differentiation in transitional cell carcinomas. *J. Clin. Pathol.* **50**, 1032–1033.

Hatina J. & Schulz W.A. (2012) Stem cells in the biology of normal urothelium and urothelial carcinoma. *Neoplasma* **59**, 728–736.

Ho P.L., Kurtova A. & Chan K.S. (2012) Normal and neoplastic urothelial stem cells: getting to the root of the problem. *Nat. Rev. Urol.* **9**, 583–594.

Hodges K.B., Lopez-Beltran A., Davidson D.D., Montironi R. & Cheng L. (2010) Urothelial dysplasia and other flat lesions of the urinary bladder: clinicopathologic and molecular features. *Hum. Pathol.* **41**, 155–162.

Liang F.-X., Bosland M., Huang H. *et al.* (2005) Cellular basis of urothelial squamous metaplasia: roles of lineage heterogeneity and cell replacement. *J. Cell Biol.* **171**, 835–844.

Mai K.T., Flood T.A., Williams P., Kos Z. & Belanger E.C. (2013) Mixed low- and high-grade papillary urothelial carcinoma: histopathogenetic and clinical significance. *Virchows Arch.* **463**, 575–581.

Mumtaz S., Hashmi A.A., Hasan S.H., Edhi M.M. & Khan M. (2014) Diagnostic utility of p53 and CK20 immunohistochemical expression in grading urothelial malignancies. *Int. Arch. Med.* **7**, 36.

Oliveira P.A., Palmeira C., Colaço A., de la Cruz L.F. & Lopes C. (2006a) DNA content analysis, expression of Ki-67 and p53 in rat urothelial lesions induced by N-butyl-N-(4-hydroxybutyl) nitrosamine ad treated with mitomycin C and bacillus Calmette-Guérin. *Anticancer Res.* **26**, 2995–3004.

Oliveira P.A., Colaço A., de la Cruz L.F., Lopes P. & Lopes C. (2006b) E-cadherin expression during urothelial carcinogenesis induced by N-butyl-N-(4-hydroxybutyl) nitrosamine in rats. *J. Exp. Clin. Cancer Res.* **25**, 425–432.

Oliveira P.A., Arantes-Rodrigues R. & Vasconcelos-Nóbrega C. (2014) Animal models of urinary bladder cancer and their application to novel drug discovery. *Expert Opin. Drug Discov.* **9**, 485–503.

Otto W., Denzinger S., Fritsche H.-M. *et al.* (2013) Introduction and first clinical application of a simplified immunohistochemical validation system confirms prognostic impact of KI-67 and CK20 for stage T1 urothelial bladder carcinoma: single-center analysis of eight biomarkers in a series of three hundred six patients. *Clin. Genitourin. Cancer* **11**, 537–544.

Palmeira C., Oliveira P.A., Arantes-Rodrigues R. *et al.* (2009) DNA cytometry and kinetics of rat urothelial lesions during chemical carcinogenesis. *Oncol. Rep.* **21**, 247–252.

Ramos D., Navarro S., Villamón R., Gil-Salom M. & Llombart-Bosch A. (2003) Cytokeratin expression patterns in low-grade papillary urothelial neoplasms of the urinary bladder. *Cancer* **97**, 1876–1883.

Reedy E.A., Heatfield B.M., Trump B.F. & Resau J.H. (1990) Correlation of cytokeratin patterns with histopathology during neoplastic progression in the rat urinary bladder. *Pathobiology* **58**, 15–27.

Shin K., Lim A., Odegaard J.I. *et al.* (2014) Cellular origin of bladder neoplasia and tissue dynamics of its progression to invasive carcinoma. *Nat. Cell Biol.* **16**, 469–478.

Vasconcelos-Nóbrega C., Colaço A., Lopes C. & Oliveira P.A. (2012) Review: BBN as an urothelial carcinogen. *In Vivo* **26**, 727–739.

Vasconcelos-Nóbrega C., Pinto-Leite R., Arantes-Rodrigues R. *et al.* (2013) *In vivo* and *in vitro* effects of RAD001 on bladder cancer. *Urol. Oncol.* **31**, 1212–1221.

Volkmer J.-P., Sashoo D., Chin R.K. *et al.* (2012) Three differentiation states risk-stratify bladder cancer into distinct subtypes. *Proc. Natl Acad. Sci. USA* **109**, 2078–2083.

Ye Y.-K., Bi X.-C., He H.-C. *et al.* (2010) CK20 and Ki-67 as significant prognostic factors in human bladder carcinomas. *Clin. Exp. Med.* **10**, 153–158.